S- and X-Band RF Feed System

P. D. Potter
Communications Elements Research Section

In support of the Mariner 1973 X-band experiment, it is necessary to implement a dual-frequency microwave feed system for the DSS 14 64-m-diameter antenna. To fulfill this requirement, a particularly attractive approach, the reflex feed system, is being implemented. The reflex feed configuration and the analytical techniques used for its analysis were described in a previous report. This article describes the calculated gain performance of the system at S-band and discusses the heating of the reflex feed dichroic reflector caused by high power S-band transmission.

I. Comparison of Measured and Computed Feed System Radiation Patterns

A cross-sectional view of the reflex feed system geometry is shown to scale in Fig. 1. The analytical technique used to predict the S-band radiation patterns of this system was described in a previous reporting (Ref. 1), and a comparison of measured and calculated radiation patterns was presented for feed configuration number 1. Figure 2 shows the final configuration (number 3) E-plane measured and calculated patterns; Fig. 3 shows the H-plane measured and calculated patterns. The analytical technique utilized for these patterns differs somewhat from that previously described in that the ellipsoid scattered fields are expanded about the Point I (Fig. 1), rather than the phase center C. By using the Point I, the flat plate is kept outside of a sphere containing all of the sources located on the ellipsoid surface and in the horn aperture. By maintaining this condition, the spherical wave expansion is rigorously correct. For the calculated patterns shown in Figs. 2 and 3, three azimuthal modes ($m = 0$, 1, and 2) and sixty polar modes were utilized.

II. Calculated Antenna Gain at S-Band

Using the digital antenna pattern (DAP) recording system in the 60-ft anechoic chamber, complete feed data were taken at the 2.295-GHz scale-model frequency. Data were taken at 1-deg increments in polar angle and 15-deg increments in azimuthal angle. After processing by the DAP software, the patterns were resolved into azimuthal Fourier component patterns, and the total pat-

tern power was calculated. Of the total pattern power, 98.8% was in the first three azimuthal modes; $m = 0$, 1, and 2. Next, the fraction of the $m = 0$, 1, and 2 mode energy intercepted by the tricone subreflector, relative to the total feed power, was calculated and defined as the forward spillover ratio. Then, each of the three m patterns was expanded in spherical waves. Each of these expansions was separately scattered off the tricone subreflector. The three scattered patterns were vectorally added and used to compute various efficiency components.

Table 1 gives the gain calculation results for the reflex feed together with a similar calculation for the present standard feed. It can be seen that the reflex feed degrades performance by approximately 0.15 dB. Almost two-thirds of this loss is due to the estimated surface deformation loss of the planar reflector. This deformation is caused by gravity and by non-uniform heating from the high power S-band transmission. The next section describes the calculated power loss profile in the flat plate which gives rise to physical distortion of the flat plate.

III. Power Loss in the Flat Plate

Because of the importance of RF heating of the flat plate and the difficulty of accurate field measurements of this effect, a new computer program, *CURENT*, has been recently completed[1] to accurately calculate the power incident on and absorbed in any general quadric surface illuminated by an arbitrary field. Near-field effects are taken account of by spherical wave techniques. Figure 4 shows the power dissipation profile in the H-plane (plane of the paper in Fig. 1) and Fig. 5 shows the profile in the E-plane. A total power of 400 kW, a frequency of 2.115 GHz, and a pure copper reflector are assumed. It can be seen that, due to the focusing action of the ellipsoid, the power dissipation is mainly in a small central "hot spot." It is presently planned that data such as those in Figs. 4 and 5 will be utilized to perform laboratory heating and surface distortion tests.

[1]By Richard Norman, JPL Communications Elements Research Section.

Reference

1. Potter, P. D., "S- and X-Band RF Feed System," in *The Deep Space Network Progress Report*, Technical Report 32-1526, Vol. VIII, pp. 53–60. Jet Propulsion Laboratory, Pasadena, Calif., Apr. 15, 1972.

Table 1. Reflex and standard feed gain, 2.295 GHz

Factor	Standard feed		Reflex feed	
	Ratio	dB	Ratio	dB
Forward spillover	0.94470	−0.2471	0.96982	−0.1331
Rear spillover	0.99738	−0.0114	0.99779	−0.0096
Non-uniform amplitude illumination	0.84207	−0.7465	0.82423	−0.8395
Non-uniform phase illumination[a]	0.97999	−0.0878	0.98408	−0.0697
Cross polarization	0.99982	−0.0008	0.99876	−0.0054
Energy ($m \neq 1$)	0.99805	−0.0085	0.97968	−0.0892
Central blockage[a]	0.94148	−0.2619	0.94195	−0.2597
Quadripod blockage	0.87498	−0.5800	0.87498	−0.5800
Paraboloid/subreflector surface tolerance loss (0.1524 cm rms)	0.97876	−0.0932	0.97876	−0.0932
Ellipsoid surface tolerance loss (0.0508 cm rms)	—	—	0.99762	−0.0103
Planar reflector Surface tolerance loss (0.1524 cm rms)	—	—	0.97876	−0.0932
Transmission loss through planar reflector (−23 dB)	—	—	0.99499	−0.0218
Total	0.62557	−2.0372	0.60191	−2.2047
Gain for 100% efficiency	2.366795 $\times 10^6$	63.7416	2.366795 $\times 10^6$	63.7416
Gain	1.480608 $\times 10^6$	61.7044	1.424590 $\times 10^6$	61.5369

[a]Phase and central blockage factors are based on a standard feed subreflector focus position of 0.928 cm in and a reflex feed subreflector position of 0.046 cm out.

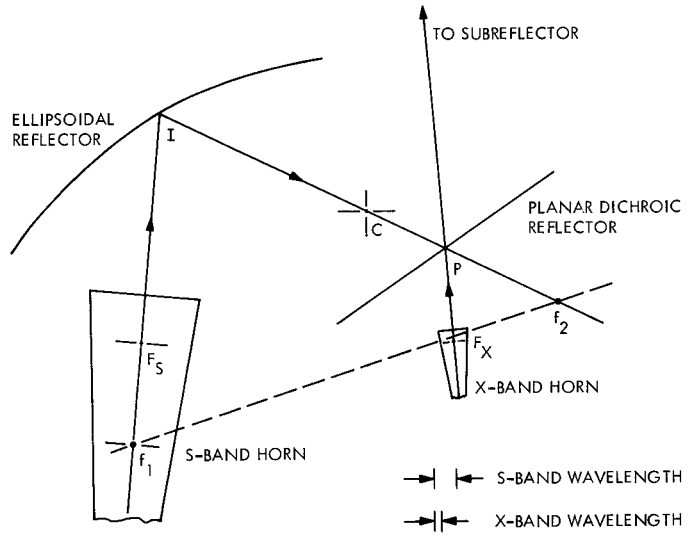

Fig. 1. Reflex feed system

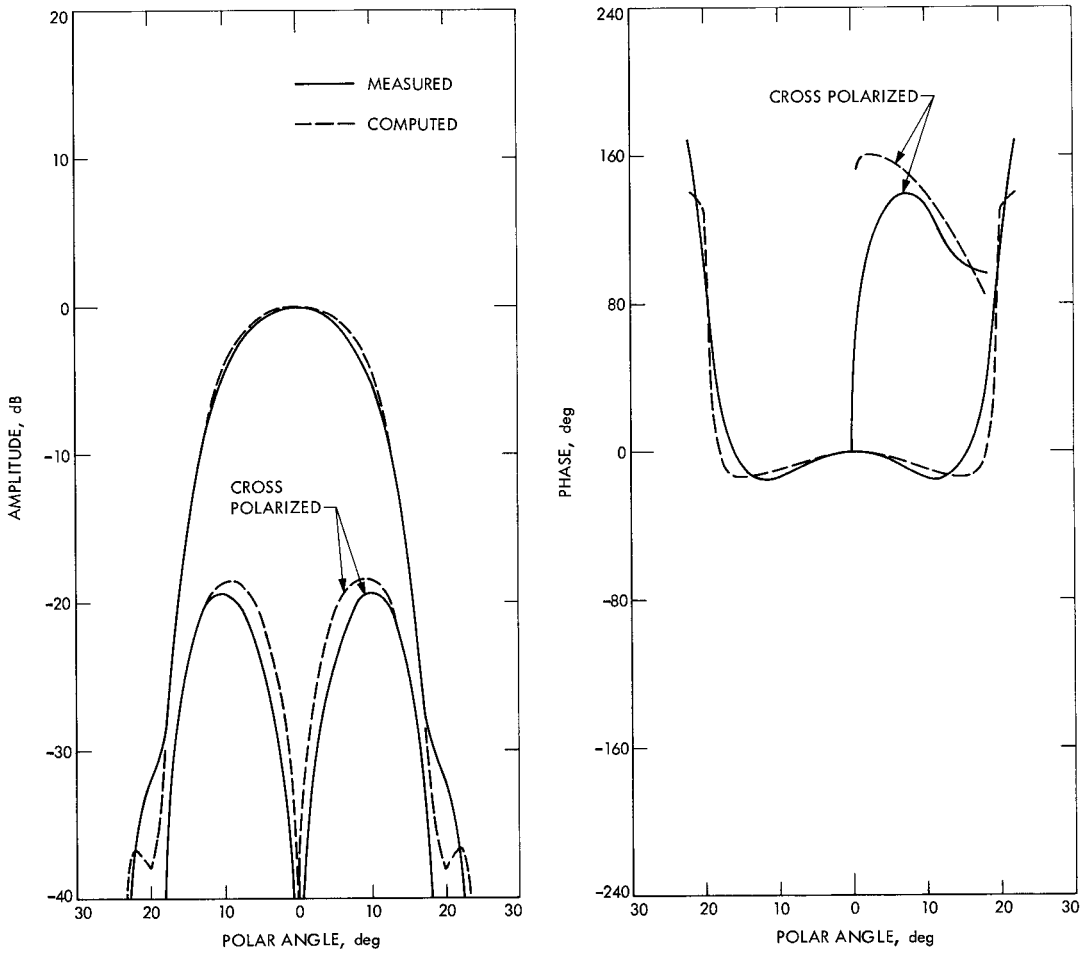

Fig. 2. E-plane reflex feed patterns

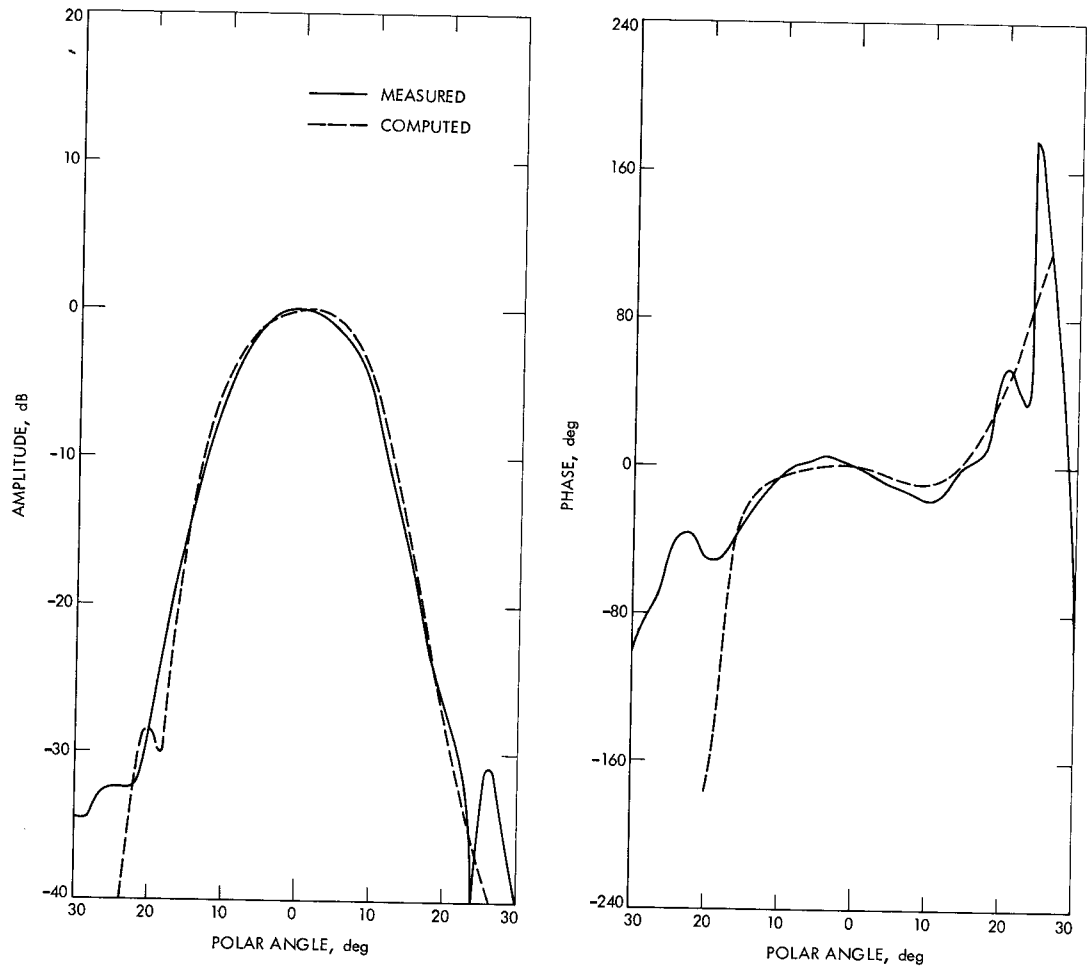

Fig. 3. H-plane reflex feed patterns

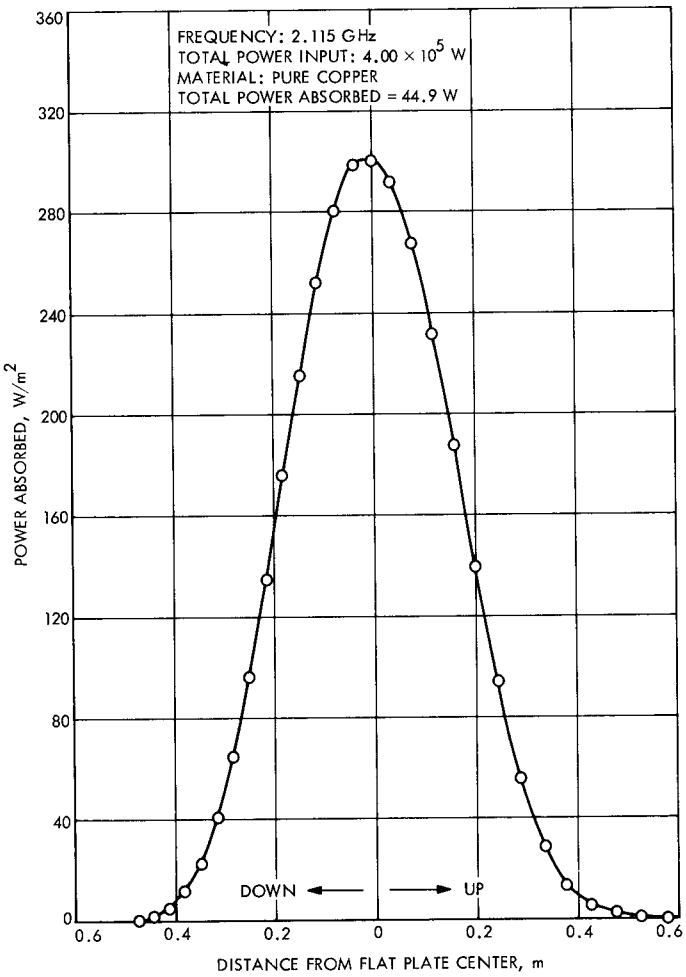

Fig. 4. H-plane flat plate power dissipation profile

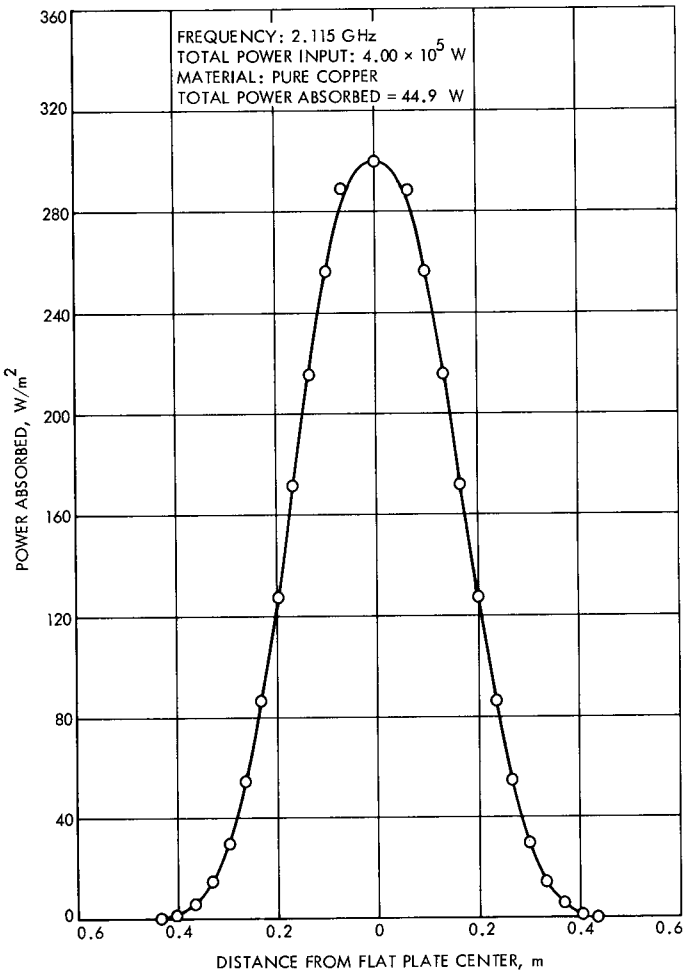

Fig. 5. E-plane flat plate power dissipation profile